Developmental Cognitive Neuroscience 76 (2025) 101638

Contents lists available at ScienceDirect

Developmental Cognitive Neuroscience

journal homepage: www.elsevier.com/locate/dcn

Intrinsic functional neurocircuitry of the bed nucleus of the stria terminalis (BNST) in early infancy

Yanbin Niu [a], M. Catalina Camacho [b], Sanjana Ravi [a], Brandon Wallroff [c], Joshua Hageman [d], Jennifer Urbano Blackford [c,e,1], Kathryn L. Humphreys [a,1,*]

[a] Department of Psychology and Human Development, Peabody College, Vanderbilt University, Nashville, TN, USA
[b] Department of Psychiatry, Washington University in St. Louis, St. Louis, MO, USA
[c] Munroe-Meyer Institute, University of Nebraska Medical Center, Omaha, NE, USA
[d] Department of Radiology and Radiological Sciences, Vanderbilt University Institute of Imaging Science, Vanderbilt University Medical Center, Nashville, TN, USA
[e] Department of Psychiatry and Behavioral Sciences, Vanderbilt University Medical Center, Nashville, TN, USA

ARTICLE INFO

Keywords:
Bed nucleus of the stria terminalis (BNST)
Anxiety
Resting state functional connectivity
Early infancy

ABSTRACT

Anxiety disorders are among the most prevalent mental health conditions, often emerging early in life and leading to substantial impairments across the lifespan. The bed nucleus of the stria terminalis (BNST) plays a central role in threat processing and anxiety regulation, yet its early functional connectivity profile and links to early signs of anxiety remain poorly understood. The current study investigates intrinsic functional connectivity of the BNST in 1-month-old infants using resting-state functional magnetic resonance imaging and explores its longitudinal association with anxiety symptoms later in infancy. We observe that early in development the BNST exhibits intrinsic connectivity with key subcortical regions, including the amygdala, hippocampus, and ventral striatum. However, connectivity patterns observed in human adults, including BNST–frontal cortex connectivity, were not observed in infants. Furthermore, weaker BNST–amygdala connectivity at 1 month was significantly associated with greater anxiety symptoms assessed at 18 months (β=-0.339, 95 % CI [-0.586, −0.093]), highlighting the potential role of early BNST connectivity in later anxiety-related behaviors. These findings provide the earliest evidence to date of BNST functional connectivity in human infancy and its prospective link to later anxiety symptoms, helping to fill a critical gap in our understanding of the early development of anxiety-related neural circuits.

1. Introduction

Anxiety disorders are among the most prevalent mental health conditions (Kessler et al., 2005), with a lifetime prevalence of approximately 34 % in the United States (Kessler et al., 2012). Anxiety disorders are associated with significant functional impairments across social, academic, and occupational domains (Aderka et al., 2012; McKnight et al., 2016; Sherbourne et al., 2010), as well as a reduced quality of life (Mendlowicz and Stein, 2000). Cross-species research has implicated the bed nucleus of the stria terminalis (BNST), a basal forebrain structure (Davis et al., 2010; Fox et al., 2015), in the expression and regulation of anxiety-related behaviors (Avery et al., 2016; Davis et al., 2010; Lebow and Chen, 2016; Walker et al., 2003). In humans, task-based fMRI studies show that the BNST is more strongly activated during unpredictable threat anticipation and exhibits altered functional connectivity with key regions such as the amygdala and medial prefrontal cortex in individuals with higher levels of anxiety (Alvarez et al., 2011; Brinkmann et al., 2018, 2017; Chavanne and Robinson, 2021; Clauss et al., 2019, 2019; Figel et al., 2019; Grogans et al., 2024; Jin et al., 2023; Klumpers et al., 2017; Meyer et al., 2019; Siminski et al., 2021; Somerville et al., 2010; Yassa et al., 2012). These findings support the BNST's role in sustained threat processing and valence surveillance—core components of anxiety neurobiology.

The BNST developmental trajectory remains poorly understood. Understanding when and how BNST connectivity emerges during early development—a critical period for shaping later emotional outcomes—may be essential for identifying the neural origins of anxiety risk. Early postnatal life is characterized by rapid brain development,

* Correspondence to: Department of Psychology and Human Development, Vanderbilt University, 230 Appleton Place, #552, Nashville, TN 37203, USA
E-mail address: k.humphreys@vanderbilt.edu (K.L. Humphreys).

[1] Kathryn L. Humphreys and Jennifer Urbano Blackford are co-senior authors

https://doi.org/10.1016/j.dcn.2025.101638

Available online 27 October 2025

during which neural circuits, including the BNST, undergo significant maturation (Halladay and Herron, 2023; Kostović et al., 2019). In rodents, BNST neurons are generated and migrate primarily during the second and third gestational weeks, corresponding to the first and second trimesters in humans (Bayer, 1987; Clancy et al., 2001). BNST connections in rodents also develop rapidly during early life. For example, BNST projections to hypothalamic nuclei mature in the early postnatal period (Lanzillo et al., 2021); connections to limbic regions, such as the medial amygdala, begin to emerge by postnatal day 5 and reach maturity by day 15 (Cooke and Simerly, 2005); and synaptic connectivity with autonomic neurons involved in visceral responses to aversive stimuli is established between postnatal days 4 and 10 (Rinaman et al., 2000). In non-human primates, white matter pathways linking the central amygdala and the lateral division of the BNST are established as early as 3 weeks of age (Oler et al., 2017). Investigating the BNST during early human life is therefore crucial for advancing our understanding of its development and maturation, including the establishment of its neural circuits and their implications for threat and stress-related responses. Despite this importance, there remains a significant gap in the literature, as few human studies to date have examined the BNST prior to childhood. Such research would provide valuable insights into the early neural origins of anxiety vulnerability, especially given that early intervention may be effective for preventing anxiety (Baughman et al., 2020).

Resting-state fMRI, which captures spontaneous neural activity in the absence of goal-directed action and external input, provides insights into intrinsic functional connectivity patterns that reflect the brain's baseline activity (Damoiseaux et al., 2006). Importantly, resting state fMRI can be collected noninvasively during natural sleep (Fransson et al., 2007), making it uniquely well-suited for studying intrinsic functional connectivity in very young populations for whom following instructions or participating in tasks is challenging. In adults, resting-state fMRI studies have demonstrated that the BNST exhibits robust functional connectivity with midline structures, including the posterior cingulate cortex, cuneus, medial frontal cortex, thalamus, and caudate, as well as limbic regions such as the amygdala and hippocampus (Avery et al., 2014; Gorka et al., 2018; Rabellino et al., 2018; Tillman et al., 2018; Torrisi et al., 2015; Weis et al., 2019). More importantly, those intrinsic BNST functional connectivity appear to be associated with anxiety- and trauma/stressor-related psychopathology (Banihashemi et al., 2022; Hofmann and Straube, 2021; Jenks et al., 2020; Pedersen et al., 2020; Rabellino et al., 2018; Torrisi et al., 2019). For example, patients with clinical anxiety showed weaker BNST resting-state functional connectivity with the dorsolateral prefrontal cortex and occipital cortex compared to non-anxious volunteers, and BNST–precuneus resting-state functional connectivity was positively correlated with anxiety symptoms (Torrisi et al., 2019). Individuals with post-traumatic stress disorder showed heightened BNST functional connectivity with the ventral and dorsal striatum compared with controls (Rabellino et al., 2018). These findings suggest that examining BNST intrinsic functional connectivity at rest may help identify neural mechanisms underlying anxiety vulnerability and symptoms. In a recent effort to explore BNST connectivity in early development, Feola et al. (2021) used resting-state functional magnetic resonance imaging (fMRI) in a sample of 8–10-year-old children. Despite developmental differences in task-based BNST activation compared to adults, intrinsic BNST connectivity in children closely resembled adult-like patterns, highlighting the establishment of BNST functional circuits by middle childhood. However, it remains unclear how early these functional circuits begin to emerge and whether early BNST connectivity relates to risk for anxiety—a gap the present study aims to address.

Infant resting-state fMRI work has largely focused on the amygdala (e.g., Filippi et al., 2021; Graham et al., 2016; Rogers et al., 2017; Salzwedel et al., 2019; Thomas et al., 2019) and/or large-scale networks (e.g., Banihashemi et al., 2023; Phillips et al., 2021), linking their connectivity to temperamental and behavioral phenotypes associated with later emotional difficulties. By contrast, BNST, as part of the extended amygdala, remains poorly understood in infancy—a critical gap given adult evidence that the BNST supports sustained threat monitoring and anxiety-related processes. Investigating BNST functional connectivity during infancy may therefore offer additional insights into the early neural substrates of emerging anxiety risk. Early-emerging temperament traits, particularly those characterized by heightened fear and anxious reactivity, have been consistently linked to increased risk for developing anxiety disorders later in life (Buss, 2011; Clauss and Blackford, 2012). These behavioral tendencies are thought to reflect individual differences in neural systems underlying threat detection and emotion regulation (Fox and Pine, 2012; Shackman and Fox, 2016). Thus, BNST functional connectivity in early infancy may be associated with temperamental risk for anxiety.

The goals of the present study were to characterize intrinsic functional connectivity of the BNST in early infancy and examine its prospective associations with later anxiety-related outcomes. Understanding the developmental timeline and functional emergence of BNST, including when its pathways are established and begin to function, has important implications for identifying the neural origins of anxiety and uncovering critical windows of vulnerability and resilience. For example, knowing when BNST connectivity with key brain regions matures could clarify how early-life experiences shape emotional regulation and threat processing. Toward this end, we collected resting-state fMRI data from 1-month-old infants and mapped the intrinsic functional connectivity of the BNST using a seed-based approach, a well-established method for examining functional connections across the brain from a defined region of interest. Based on Feola et al. (2021) findings in children and evidence that large-scale functional networks are already present at birth (Doria et al., 2010; Fransson et al., 2007; Nielsen et al., 2023), we hypothesized that the BNST would exhibit functional connectivity with key regions (e.g., the amygdala) as early as 1 month of age, though its connectivity might not yet fully resemble the adult pattern. Furthermore, we explored whether intrinsic BNST connectivity at 1 month could predict anxiety risk assessed later in infancy. To our knowledge, this is the first neuroimaging study to examine BNST functional connectivity in human infants. As such, we did not have strong *a priori* hypotheses regarding whether specific connections would be predictive. If associations between early BNST connectivity and later anxiety risk were observed, this would suggest that individual differences in BNST circuitry contribute to emerging anxiety risk even within the first months of life. Conversely, null findings would suggest that the functional relevance of BNST connectivity for anxiety symptoms may emerge later in development.

2. Methods

2.1. Participants and procedures

Families were recruited during pregnancy from the greater Nashville area through obstetrics clinics and social media advertisements for the longitudinal study of infant brain and behavioral development (Ravi et al., 2023). Interested individuals were first screened via phone to confirm eligibility, which included being 18 years or older, currently pregnant with a singleton pregnancy, fluent in English, a U.S. citizen or permanent resident, and having no immediate plans to move out of the greater Nashville area. After their due date, participants were screened again to assess their infant's eligibility for MRI scanning. Exclusion criteria included parent-reported severe complications during birth, infant head trauma, premature birth (prior to 36 weeks gestation), and any infant MRI contraindications (e.g., metal implants). All study procedures were approved by the Vanderbilt University Institutional Review Board. Informed consent was obtained from all participants, including consent for their infant's participation following birth. Eligible infants underwent MRI scanning during natural sleep (see detailed MRI collection procedures section). Mother–children dyads were subsequently invited back for a follow-up assessment at child age 6 months and 18 months during which parents were asked to complete a battery of questionnaires. Study data were collected and managed using REDCap electronic data capture tools hosted at Vanderbilt University (Harris et al., 2019, 2009). Participants were compensated $25 per hour for their participation at each time point.

The study included 107 participants who had any resting-state fMRI data collected and successfully acquired structural MRI (either T1- or T2-weighted) at 1 month of age. After preprocessing, functional scans with at least 4 min of low motion data were retained, resulting in 99 datasets for functional connectivity analysis. Following seed-to-whole-brain functional connectivity analysis, we engaged in additional quality checks to ensure all included had clear, low motion images; this resulted in the exclusion of 39. Our final sample size of 60 infants were retained for subsequent functional analyses. There were no statistically significant demographic differences between participants included in the analyses and those excluded. See Table 1 for sample characteristics.

2.2. Fear

Parents completed the Infant Behavior Questionnaire-Short Form Revised (IBQ-SF-R) (Putnam et al., 2014) at 6 months of age. This 91-item questionnaire has demonstrated excellent interrater and test-retest reliability (Putnam et al., 2014) and comprises 13 subscales which assess infants' tendencies toward reactivity, emotionality, and regulation. For the present analyses, we focused on the fear subscale as an indicator of early anxiety-related phenotypes. The fear subscale comprises six items that assess infants' responses to unfamiliar or potentially threatening situations, with example items including behaviors like clinging to a caregiver or refusing to approach an unfamiliar adult when introduced to an unfamiliar adult. In the current sample, Cronbach's alpha for the fear was 0.80, indicating good internal consistency.

2.3. Anxiety symptoms

Child anxiety symptoms were assessed at 18 months using the brief early childhood screening assessment (ECSA). The ECSA is a 22-item, caregiver-report measure designed to assess early emotional and behavioral difficulties, including anxiety symptoms in young children aged 18–60 months (Fallucco et al., 2017). To develop a robust measurement model for anxiety symptoms, we identified items with conceptual relevance to anxiety and conducted both exploratory factor analysis (EFA) and confirmatory factor analysis (CFA). First, based on the conceptual relevance of the items, we identified item 11 ("is easily startled or scared"), item 14 ("is clingy, does not want to separate from parent"), and item 15 ("seems nervous or worries a lot") as anxiety-related items. To ensure no relevant items were overlooked, we employed EFA with models specifying two to eight factors. Only in the two-factor EFA, items 11, 14, and 15 loaded onto a single latent structure, along with items 4 ("avoids situations that remind of scary events"), 12 ("has trouble interacting with other children"), and 21 ("has unusual repetitive behaviors [rocking, flapping]") (see Supplementary Materials for detailed factor loadings). Item 12 was excluded due to a low factor loading (< 0.35). We next conducted CFA using the retained items (4, 11, 14, 15, and 21) to evaluate the latent structure. However, item 21 had a negative loading (-0.036) and a relative low variance estimate (0.019), and thus was subsequently removed. A revised CFA was conducted using items 4, 11, 14, and 15, and demonstrated excellent model fit, as indicated by a nonsignificant chi-square test, $\chi^2(2) = 0.079$, $p = 0.961$, a Comparative Fit Index (CFI) of 1.000, a Tucker-Lewis Index (TLI) of 1.343, and a Root Mean Square Error of Approximation (RMSEA) of 0.000. The Standardized Root Mean Square Residual (SRMR) was also minimal at 0.009. All retained items (4, 11, 14, and 15) demonstrated significant standardized factor loadings (item 15: 0.541, item 14: 0.487, item 11: 0.652, and item 4: 0.559), supporting the convergent validity of the latent construct. The variance estimates for the items ranged from 0.125 to 0.190, indicating that the items consistently contributed to the latent anxiety factor (see Supplementary Materials for detailed factor analyses results). In the current sample, Cronbach's alpha for anxiety problems was 0.64, indicating acceptable internal consistency.

Table 1
Sample demographic characteristics.

Infant sex n (%)	31 males (52%)
Infant age at scan (Mean, SD, range)	4.71, 0.85, 3.43–6.86 weeks
Infant race n (%)	
American Indian or Alaska Native	0 (0 %)
Asian	2 (3 %)
Black or African American	3 (5 %)
Native Hawaiian or Other Pacific Islander	0 (0 %)
White	50 (83 %)
Other	5 (8 %)
Infant ethnicity n (%)	5 Hispanic/Latinx (8 %)
Caregiver education n (%)	
High school graduate or equivalent	1 (2 %)
Trade/technical/vocational training	1 (2 %)
Some college credit, no degree	4 (7 %)
Associate's degree	2 (3 %)
Bachelor's degree	18 (30 %)
Graduate degree	33 (55 %)
Other	1 (2 %)
Income-to-needs ratio (Mean, SD, range)	1.70, 0.77, 0.08–2.85

2.4. MRI acquisition

MR images were acquired at approximately one month of age at the Vanderbilt University Institute of Imaging Science (VUIIS) Center for Human Imaging using a Philips Ingenia Elition 3.0 T equipped with a 32-channel head coil. Infants were prepared using the "swaddle and soothe" method and scanned during natural sleep in the evenings (for more details, see Camacho et al., 2020). Families arrived at the imaging suite typically between 5:30 pm and 7:30 pm. The infant was changed into a disposable diaper and swaddled using a muslin blanket before being wrapped by a MedVac immobilizer designed for infants. The infant was then fitted with hearing protection which included placing silicone ear putty in their ears secured with skin-safe medical tape and covering their ears with Natus MiniMuffs (Styrofoam pads with adhesives) for additional noise reduction. Parents were then encouraged to feed and put their infant to sleep. Once asleep, the infant was transferred to the scanner bed and slim-fit headphones playing pink noise intermixed with rain sounds were placed on their ears. The infant's head and the headphones were secured with foam pads to fill out the head coil space and reduce likelihood of motion during scanning. If the infant remained soundly asleep, acquisition was initiated, otherwise the infant was given additional time to move back into a deep sleep before starting the scan. A trained research assistant monitored the infant during the scan and alerted the scan technician if the infant woke up. If the infant woke up, the researcher soothed them back to a deep sleep before resuming the scan. This process was repeated until either all data were collected, or the family decided to end the session.

Relevant to the present study, collected modalities included a T1-weighted anatomical image (TR=10 ms, TE=4.6 ms, TI=700 ms, flip angle=8°, FOV=256x256x150 mm, resolution=1x1x1 mm^3), T2-weighted anatomical image (TR=2500 ms, TE=310 ms, flip angle=90°, FOV=220x220x144 mm, resolution=0.8 ×0.8 ×0.8 mm^3), and resting-state fMRI (resolution=2.0 ×1.9 ×1.9 mm^3, 54 axial slices, 96 ×96 acquisition matrix, flip angle=60°, TR=1410 ms, TE=30 ms, 3 simultaneous slices, 270 continuous volumes). Framewise Integrated Real-time MRI monitoring (FIRMM) software was installed by VUIIS partway through data collection and was used to monitor motion in real time for the resting-state scan and the sequence was repeated until approximately 10-minutes of fMRI data under 0.2 mm framewise displacement was collected or until the scan was ended. All MR images were visually inspected for artifacts prior to processing.

2.5. MRI processing

We preprocessed the anatomical and functional data using NiBabies 23.1.0, derived from fMRIPrep (Esteban et al., 2019). The underlying workflow engine used was Nipype 1.8.6 (Esteban et al., 2022; Gorgolewski et al., 2011).

2.5.1. Anatomical data preprocessing

The T1-weighted (T1w) and T2-weighted (T2w) images were denoised and corrected for intensity non-uniformity (INU) with N4BiasFieldCorrection (Tustison et al., 2010), distributed with ANTs (Avants et al., 2008). The T2w-reference was then skull-stripped with a modified implementation of the antsBrainExtraction.sh workflow (from ANTs), using UNCInfant:cohort-1 as target template. Brain tissue segmentation of cerebrospinal fluid (CSF), white-matter (WM) and gray-matter (GM) was performed on the brain-extracted T1w using FSL FAST. Volume-based spatial normalization to one standard space (MNIInfant) was performed through nonlinear registration with antsRegistration ANTs, using brain-extracted versions of both T1w reference and the T1w template. The following template was selected for spatial normalization and accessed with TemplateFlow: MNI Unbiased nonlinear Infant Atlases 0–4.5 yr (Fonov et al., 2009).

2.5.2. Functional data preprocessing

A B0-nonuniformity map (i.e., fieldmap) was estimated based on two (or more) echo-planar imaging (EPI) references with topup (Andersson et al., 2003). For each of the BOLD runs, the following preprocessing was performed. Head-motion parameters with respect to the BOLD reference (transformation matrices, and six corresponding rotation and translation parameters) were estimated before any spatiotemporal filtering using mcflirt (FSL; Jenkinson et al., 2002). The estimated fieldmap was then aligned with rigid-registration to the target EPI reference run. The field coefficients were mapped onto the reference EPI using the transform. BOLD runs were slice-time corrected to 0.666 s (0.5 of slice acquisition range 0s-1.33 s) using 3dTshift from AFNI (Cox and Hyde, 1997). The BOLD reference was then co-registered to the T1w reference using bbregister (FreeSurfer; Zöllei et al., 2020) which implements boundary-based registration (Greve and Fischl, 2009). Co-registration was configured with six degrees of freedom. Several confounding time-series were calculated based on the preprocessed BOLD: framewise displacement (FD), DVARS and three region-wise global signals. FD and DVARS were calculated for each functional run, both using their implementations in Nipype (following the definitions by Power et al., (2014)). The three global signals were extracted within the CSF, the WM, and the whole-brain masks. The BOLD time-series were resampled into standard space, generating a preprocessed BOLD run in MNIInfant: cohort-1 space. All resamplings can be performed with a single interpolation step by composing all the pertinent transformations (i.e., head-motion transform matrices, susceptibility distortion correction when available, and co-registrations to anatomical and output spaces). Gridded (volumetric) resamplings were performed using antsApplyTransforms (ANTs), configured with Lanczos interpolation to minimize the smoothing effects of other kernels (Lanczos, 1964).

The eXtensible Connectivity Pipeline-DCAN (XCP-D) (Ciric et al., 2018; Satterthwaite et al., 2013) was used to post-process the outputs of nibabies. XCP-D was built with Nipype version 1.8.6 (Esteban et al., 2022; Gorgolewski et al., 2011). Native-space T1w images were transformed to MNIInfant space at 1 mm^3 resolution. For each of the BOLD runs found, the following post-processing was performed. Volumes with FD greater than 0.2 mm were flagged as high-motion outliers for the sake of later censoring (Power et al., 2014). In total, 36 nuisance regressors were selected from the preprocessing confounds, according to the '36 P' strategy. These nuisance regressors included six motion parameters, mean global signal, mean white matter signal, mean cerebrospinal fluid signal with their temporal derivatives, and quadratic expansion of six motion parameters, tissue signals and their temporal derivatives (Ciric et al., 2018; Satterthwaite et al., 2013). Regression of global signal shifts connectivity correlations across the brain from positive values to being centered at approximately zero (Murphy et al., 2009; Murphy and Fox, 2017) and thus negative correlations should be interpreted as relatively less connectivity as opposed to negative connectivity. Finally, linear trend and intercept terms were added to the regressors prior to denoising. The BOLD data were despiked with AFNI's 3dDespike. Nuisance regressors were regressed from the BOLD data using linear regression, as implemented in Nilearn. Any volumes censored earlier in the workflow were then interpolated in the residual time series produced by the regression. The interpolated timeseries were then band-pass filtered using a(n) second-order Butterworth filter, in order to retain signals between 0.01 and 0.1 Hz. The filtered, interpolated time series were then re-censored to remove high-motion outlier volumes. No spatial smoothing was applied. For the final processed data, the mean FD was 0.11 mm, and the mean scan length was 9.84 min after censoring (range 4.04–14.85 min).

2.6. Seed-to-whole-brain functional connectivity analysis

The BNST was manually traced on the 0–2 month MNI infant template. BNST tracing was guided by Theiss et al. (2017) and adapted for newborn brain structure (see Fig. 1). The BNST was first traced on the T2w image and visually confirmed with the T1W image. The mask was traced in the coronal view, with the axial and sagittal views used for confirmation. The definition of the BNST was based on the presence of gray matter (determined by voxels intensity) within a space defined by several anatomical landmarks. The inferior boundary was based on the superior aspect of the anterior commissure. The medial and lateral boundaries were defined by the fornix and internal capsule, respectively. The posterior boundary was defined by the interventricular foramen, the channel that forms between the lateral ventricles and third ventricle. BNST tracings were performed independently by two tracers who were both highly reliable in tracing the BNST in adults (co-author BW and second-to-last senior author JUB). The final mask was based on consensus across both tracers. The mask was visually confirmed on a subset of T2w scans of participants in this sample. This BNST mask was subsequently used as the seed region for the seed-to-whole-brain functional connectivity analysis. For each subject, the mean time series was extracted from all voxels within the BNST seed region. Additionally, the voxel-wise time series across the entire brain was extracted. Pearson correlation coefficients were then computed between the time series of the BNST seed and the time series of each voxel across the brain, resulting in voxel-wise correlation maps. No spatial smoothing was applied. These correlation maps were subsequently Fisher-z transformed. Second-level group analyses were conducted in Nilearn v0.10.0. We fit GLMs and computed the second-level contrast with SecondLevelModel (smoothing_fwhm = 4.0). A 4 mm FWHM isotropic Gaussian kernel was applied to enhance statistical robustness—improving SNR, stabilizing variance, and tolerating minor misregistration—and to better meet the smoothness assumptions underlying clusterwise inference (Rosenfeld, 1976; Worsley et al., 1996; Worsley and Friston, 1995). We then thresholded the second-level statistical images using Nilearn's threshold_stats_img with Bonferroni-corrected voxelwise control ($\alpha = 0.001$). For visualization only, we also display FDR thresholded maps (see Fig. 2). All subsequent processing and analyses were based on the Bonferroni-thresholded maps. The resulting thresholded map was then entered to FSL v6.0.5 (Jenkinson et al., 2012) 'cluster' to further identify clusters and generate reports on cluster size, location, and peak coordinates. Moreover, cluster-size thresholds were determined using AFNI's 3dttest++ with 3dClustSim (Cox et al., 2017a, 2017b), which simulates noise volumes by randomizing and permuting input datasets, without relying on a

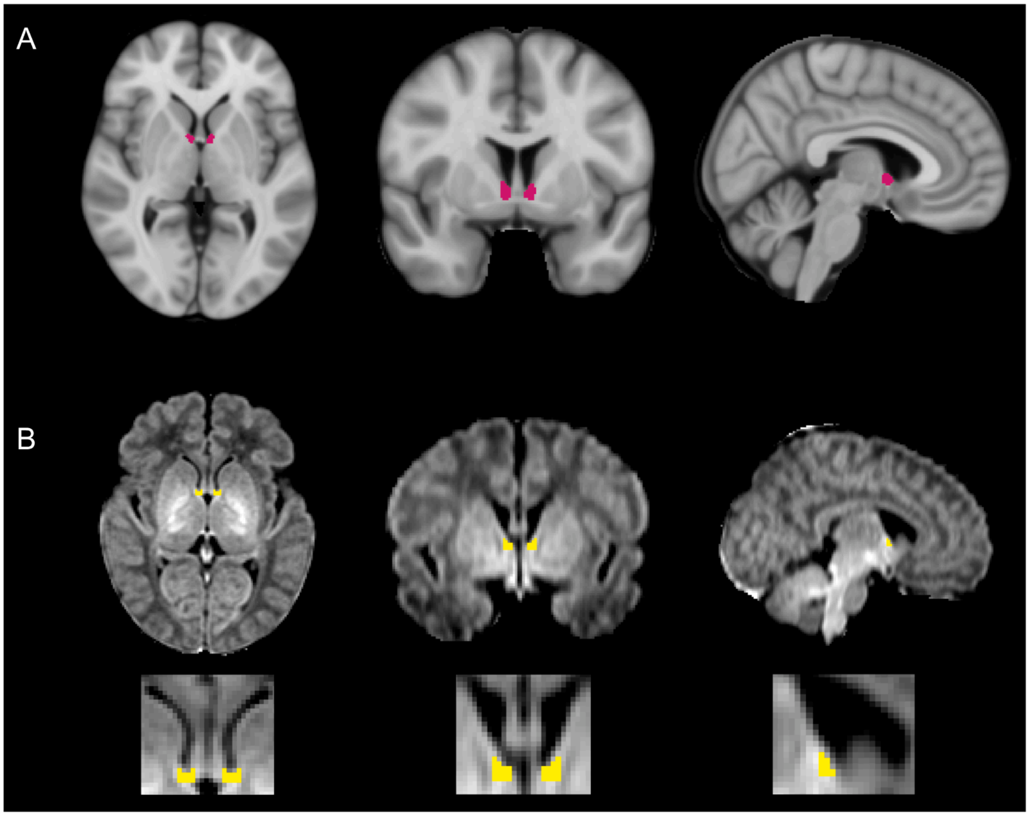

Fig. 1. The human bed nucleus of the stria terminalis (BNST) masks. A. Adult BNST mask at a 10 % threshold from a probabilistic BNST mask (Theiss et al., 2017); this panel is for visual comparison with adult anatomy only (not used for alignment or analysis). B. BNST mask in 1-month-old infants, displayed in the 0–2-month-old infant MNI atlas space. See Supplementary Fig. S1 for all relevant slices across coronal, axial, and sagittal views.

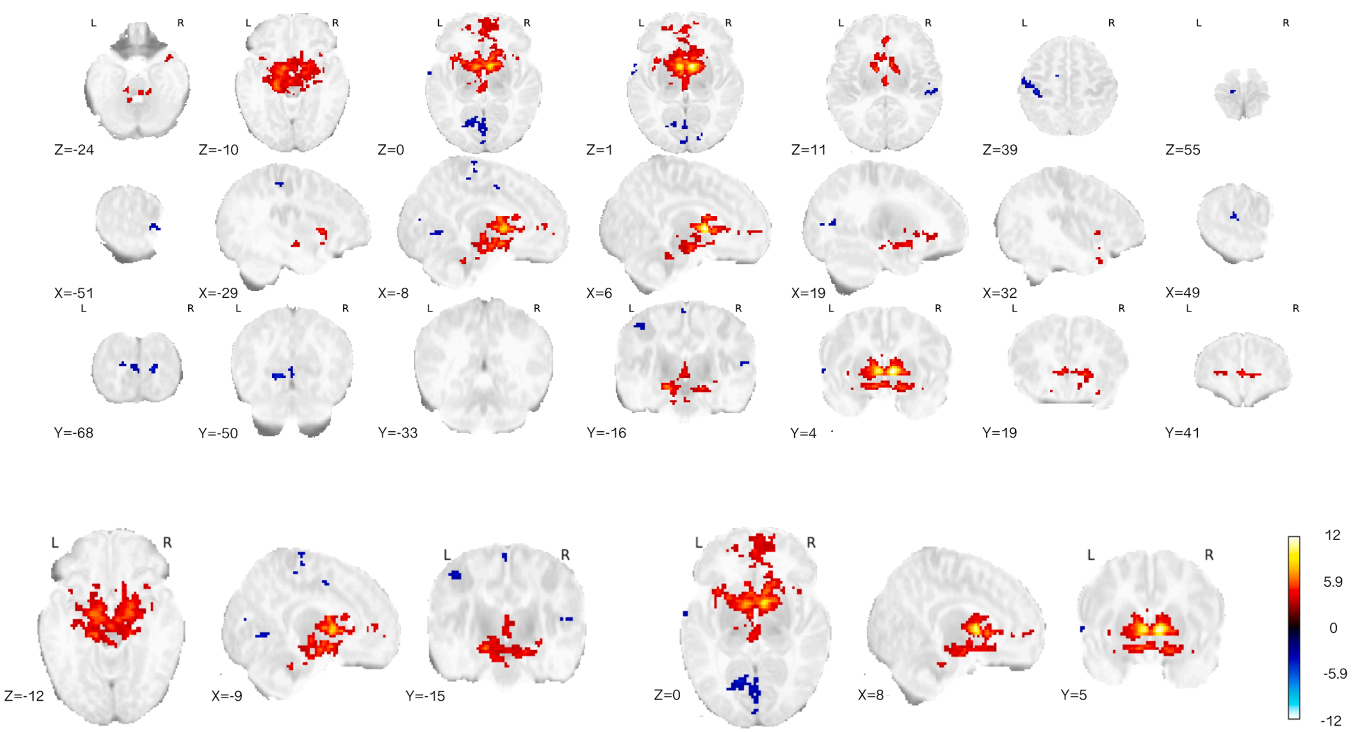

Fig. 2. Whole-brain resting-state functional connectivity seeding from the bed nucleus of the stria terminalis in 1-month-old infants. For visualization purposes, functional connectivity patterns are displayed following false discovery rate correction for multiple comparisons at the voxel-wise level ($p < 0.05$). It is important to note that this correction was applied only for presentation and was not used in the formal statistical analyses.

predefined spatial autocorrelation function (ACF) model. Cluster inference was performed with a voxel-wise threshold of $p < 0.001$ and a cluster-level significance threshold of $p < 0.05$. Based on the simulations, clusters containing four or more voxels were considered statistically significant.

For each significant cluster, the ConnectivityMeasure function from Nilearn v0.10.0 was utilized to compute the seed-to-cluster (BNST-to-cluster) correlation coefficient for each subject. The resulting subject-level correlation coefficients were then Fisher-z transformed to obtain seed-to-cluster functional connectivity estimates to use in further behavioral correlation analyses.

2.7. Analytic plan

Statistical analyses were conducted using R v4.3.3 (R Core Team, 2013). All variables were z-scored prior to analyses to facilitate comparisons between variables and improve the interpretability of results (Gelman, 2008). We examined the associations between each of the post hoc seed-to-cluster functional connectivity and behavioral measurements (e.g., fear and anxiety symptoms). Covariates included average motion (i.e., mean FD after censoring), corrected infant age at the time of the scan, and infant sex. Linear modeling was performed using the "lavaan" package with a robust maximum likelihood ("MLR") estimation (Huber, 1967; White, 1982). Within the final dataset for BNST functional connectivity ($N = 60$), missing data were addressed using Full Information Maximum Likelihood (FIML), which utilizes all available data points, including those with partial information, to estimate model parameters and maximize the use of the dataset (Arbuckle, 2013). Outliers were handled using the Winsorize function in the "DescTools" package in R, with the default thresholds of the 5th and 95th percentiles. statistical tests were two-tailed, with an alpha level of 0.05. The Benjamini-Hochberg correction was applied at a false discovery rate (FDR) of 0.05 using the "stats" package in R in order to account for multiple comparisons.

3. Results

3.1. BNST whole-brain functional connectivity

The BNST whole-brain functional connectivity analysis demonstrated four statistically significant clusters, including the left amygdala (Cluster 1), left hippocampus (Cluster 2), right ventral striatum (Cluster 3), and right amygdala (Cluster 4) (see Table 2, Fig. 3). The average functional connectivity values between the BNST and each cluster were as follows: BNST–left amygdala (M = 0.183, SD = 0.155), BNST–left hippocampus (M = 0.367, SD = 0.185), BNST–right ventral striatum (M = 0.261, SD = 0.190), and BNST–right amygdala (M = 0.045, SD = 0.169) (see Fig. 4).

Table 2
Statistically significant clusters of whole-brain functional connectivity from bed nucleus of the stria terminalis (BNST) seeds.

Region	Number of voxels	Extent mm^3	Peak T-stat	Coordinates X	Y	Z
Left amygdala	19	152	6.61	47	73	31
Left hippocampus	17	136	6.82	43	64	31
Right ventral striatum	9	72	6.54	55	78	36
Right amygdala	6	48	6.30	59	71	30

Note: Extent refers to the volume of the cluster, measured in mm^3. Coordinates is the spatial location of the center of the mask in template space, represented by the X, Y, and Z coordinates.

3.2. Associations between BNST functional connectivity and fear scores at 6 months

We examined the associations between the clusters that showed significant positive BNST connectivity and fear scores at age 6 months, as measured via IBQ-SF-R fear subscale. All associations between BNST connectivity and IBQ fear were small in magnitude and not statistically significant (see Fig. 5; BNST–left amygdala: $\beta = 0.086$, 95 % CI [-0.226, 0.397], $p = 0.591$; BNST–left hippocampus: $\beta = -0.121$, 95 % CI [-0.381, 0.138], $p = 0.359$; BNST–right ventral striatum: $\beta = 0.123$, 95 % CI [-0.124, 0.371], $p = 0.329$; BNST–right amygdala: $\beta = -0.055$, 95 % CI [-0.326, 0.217], $p = 0.694$).

3.3. Associations between BNST functional connectivity and anxiety symptoms at 18 months

We next investigated whether BNST functional connectivity at 1 month, across the 4 identified clusters, was associated with anxiety symptoms at age 18 months (see Fig. 6). Lower BNST–left amygdala connectivity at 1 month was significantly associated with higher anxiety symptoms at 18 months ($\beta = -0.339$, 95 % CI [-0.586, −0.093], $p = 0.007$ ($p_{corrected} = 0.028$)). The associations between BNST functional connectivity with the other clusters and later anxiety symptoms were negative, small in effect size, and not statistically significant (BNST–left hippocampus: $\beta = -0.193$, 95 % CI [-0.453, 0.067], $p = 0.145$; BNST–right ventral striatum: $\beta = -0.111$, 95 % CI [-0.304, 0.083], $p = 0.264$; and BNST–right amygdala: $\beta = 0.010$, 95 % CI [-0.327, 0.347], $p = 0.954$).

To evaluate whether socioeconomic status may have influenced the findings, we reconducted all primary models with income-to-needs ratio as a covariate. Results from these models were nearly identical to those presented in the manuscript, leaving our conclusions unchanged.

4. Discussion

In the current study, we examined the intrinsic functional connectivity of the BNST in 1-month-old infants using resting-state fMRI, as well as its prospective association with anxiety risks later in infancy—measured at 6 months using the fear subscale from the IBQ-SF-R and at 18 months using the anxiety factor from the ECSA. We identified two main findings. First, the BNST exhibited intrinsic functional connectivity with key subcortical regions—including the bilateral amygdala, left hippocampus, and right ventral striatum—as early as 1 month of age. However, we did not observe significant BNST connectivity with other regions (e.g., frontal cortex) at this age, suggesting an ongoing developmental process in which long-range connections may not yet be fully established. Second, individual differences in BNST–left amygdala connectivity at 1 month were prospectively associated with anxiety symptoms at 18 months, but not with fear-related temperament at 6 months. This pattern suggests that reduced coordinated communication between the BNST and amygdala may be associated with greater susceptibility to anxiety, while the absence of a similar association at 6 months may reflect developmental timing and/or differences between temperament-based and symptom-based assessments.

We discovered that 1 month of age, the BNST exhibits connectivity with subcortical regions, including the amygdala, hippocampus, and ventral striatum, which aligns with prior findings in youth (Feola et al., 2021) and adults (Avery et al., 2014; Gorka et al., 2018; Tillman et al., 2018; Torrisi et al., 2015; Weis et al., 2019). The current finding extends our knowledge of BNST functional connectivity in humans by demonstrating that BNST connectivity with key subcortical regions begins to emerge remarkably early in development. BNST–amygdala functional connectivity at rest has been extensively documented in adults (Avery et al., 2014; Birn et al., 2014; Gorka et al., 2018; Oler et al., 2012; Tillman et al., 2018; Torrisi et al., 2015; Weis et al., 2019), as well as evidence of their structural connections (Avery et al., 2014; Krüger

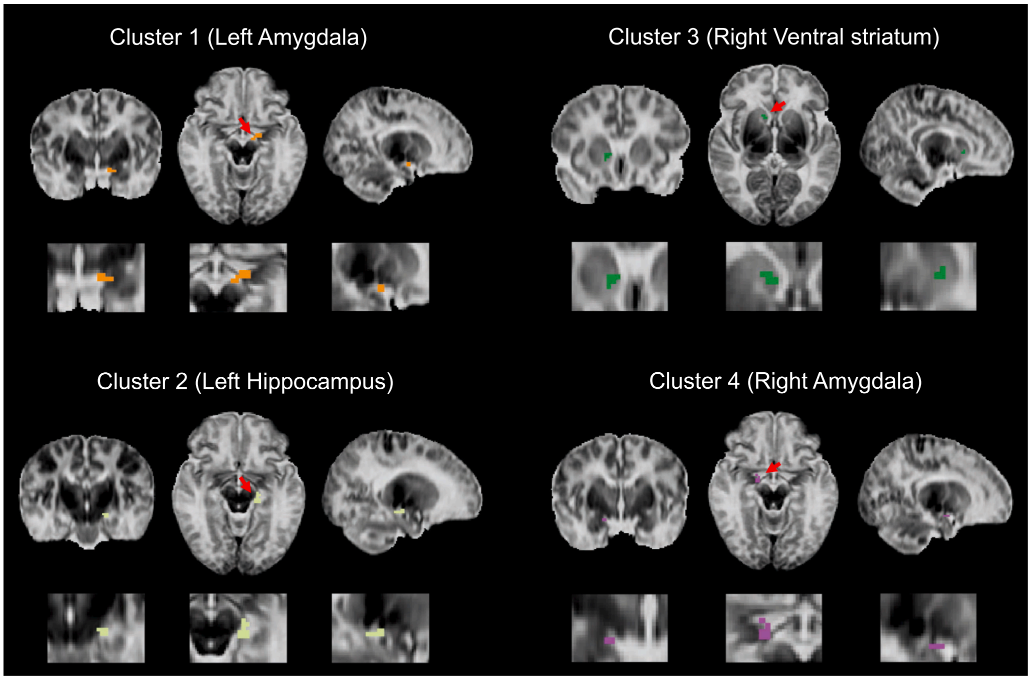

Fig. 3. Four clusters identified through whole-brain resting-state functional connectivity analysis seeding from the bed nucleus of the stria terminalis (BNST). The four clusters identified include the left amygdala, left hippocampus, right ventral striatum, and right amygdala.

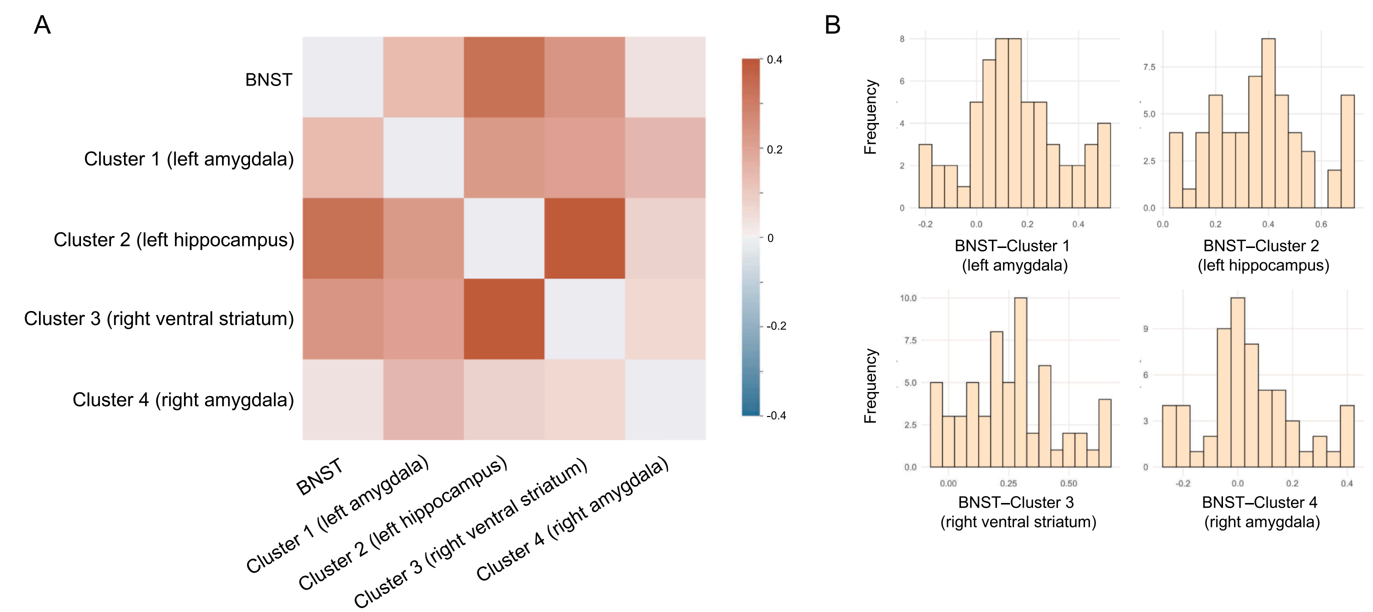

Fig. 4. Mean functional connectivity between the bed nucleus of the stria terminalis (BNST) and the identified clusters. A. Mean functional connectivity between the BNST and the identified clusters, including the left amygdala, left hippocampus, right ventral striatum, and right amygdala. B. Distribution of functional connectivity between the BNST and the identified clusters, presented as histograms.

et al., 2015; Mori and Aggarwal, 2014; Oler et al., 2017). Furthermore, the observed functional connectivity between the BNST and the bilateral amygdala in 1-month-old infants likely reflects connections with the central nucleus of the amygdala (CeA), as the identified cluster is located in central, medial regions of the amygdala. The BNST and CeA are two highly interconnected structures in animal studies that form key components of the central extended amygdala (Alheid and Heimer, 1988; de Olmos and Heimer, 1999), playing a critical role in threat-related processing and stress responses (Davis et al., 2010; Fox et al., 2015; Fox and Shackman, 2019). The BNST and CeA are connected via two primary pathways—the stria terminalis and the ventral amygdalofugal pathway—which together support bidirectional communication (Nauta and Nauta, 1993) and enable the integration of sensory, contextual, and emotional information (Shackman and Fox, 2016). Animal studies also suggest these pathways develop early in postnatal life (Oler et al., 2017). For example, using *in vivo* diffusion-weighted imaging and resting-state fMRI techniques, Oler et al. (2017) demonstrated in a longitudinal study of monkeys (ages 3 weeks and 7 weeks) that the stria terminalis and ventral amygdalofugal pathways are already in place by 3 weeks of age. Additionally, intrinsic functional connectivity between the lateral BNST and the CeA showed a marked increase in coherence between 3 and 7 weeks of age. Our findings now extend this understanding to human

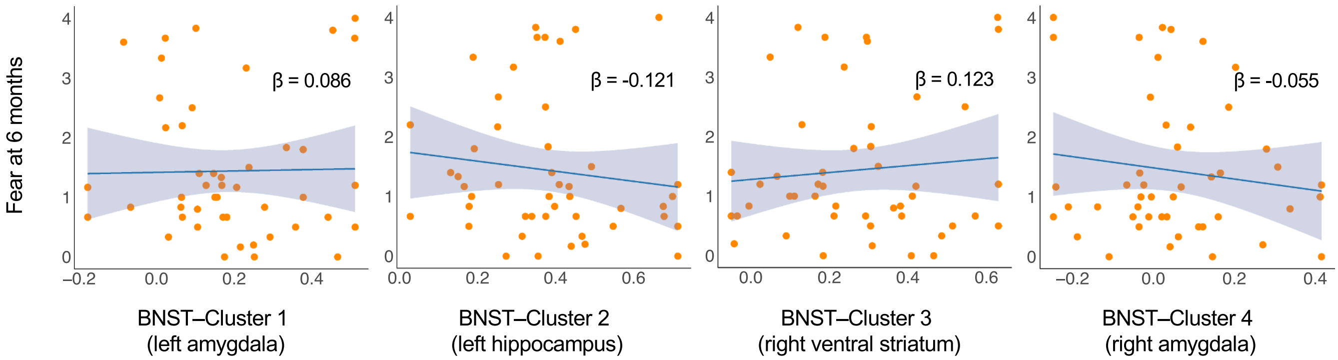

Fig. 5. Scatterplots of fear scores at 6 months with functional connectivity between the bed nucleus of the stria terminalis (BNST) and four identified clusters at age 1 month.

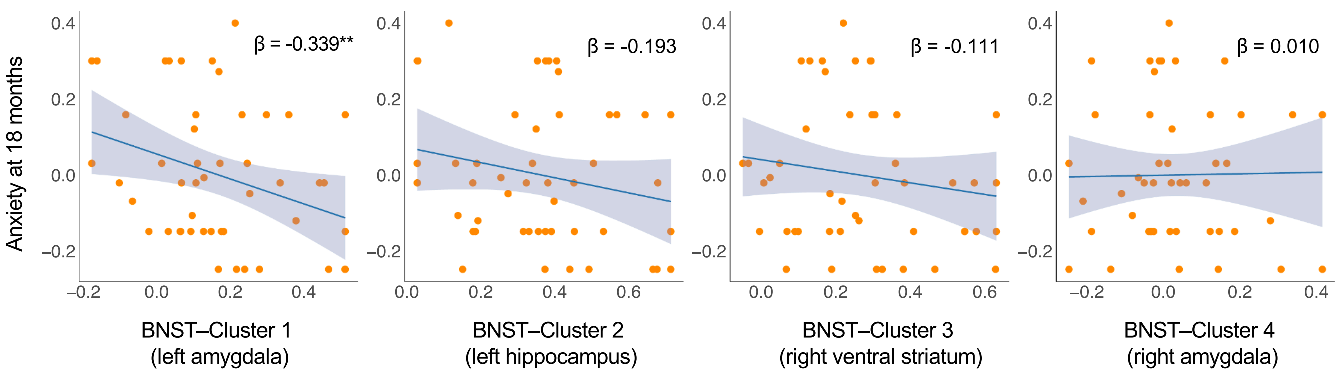

Fig. 6. Scatterplots of anxiety at 18 months with functional connectivity between the bed nucleus of the stria terminalis (BNST) and four identified clusters at age 1 month.

development, revealing that this key threat-processing circuit is established by 1 month of age.

In addition to its connectivity with the amygdala, the BNST also exhibited intrinsic functional connectivity with the hippocampus and ventral striatum in 1-month-old infants. Invasive tract-tracing studies in rodents have demonstrated that the hippocampus directly projects to BNST (Bienkowski et al., 2018; Dong et al., 2001a; Dong and Swanson, 2006; Myers et al., 2014; Swanson and Cowan, 1977), which plays a critical role in integrating contextual information related to sustained threats (Lebow and Chen, 2016). Similarly, connectivity between the BNST and the hippocampus has been documented in both non-human primates (Berry et al., 2022; Fox et al., 2018), human children (Feola et al., 2021), and human adults (Avery et al., 2014; Gorka et al., 2018; Tillman et al., 2018; Torrisi et al., 2015; Weis et al., 2019). Moreover, the hippocampal cluster identified in the current study was localized more specifically to the anterior CA region, rather than its posterior segment, replicating a pattern observed in adult populations (Avery et al., 2014; Feola et al., 2021; Tillman et al., 2018; Torrisi et al., 2015). The anterior hippocampus is critically involved in integrating contextual information with emotional valence, facilitating the association of environmental contexts with specific emotional experiences (Zeidman and Maguire, 2016), and plays a central role in high-level cognitive functions and emotional responses (Strange et al., 2014). Additionally, the BNST's connectivity with the ventral striatum observed in 1-month-old infants is also noteworthy. In rodents, the BNST connects to ventral striatum, particularly the nucleus accumbens (NAcc) (Dong et al., 2001b; Dong and Swanson, 2004, 2003; Shin et al., 2008). Moreover, human diffusion imaging studies show structural connectivity between the BNST and NAcc (Avery, 2014) and highlight that fiber pathways from the BNST to the medial prefrontal cortex traverse through the head of the caudate and NAcc (Krüger et al., 2015). Resting-state studies in humans have also demonstrated BNST functional coupling with ventral striatal regions at rest, including the NAcc, caudate, and putamen (Avery et al., 2014; Feola et al., 2021; Gorka et al., 2018; Torrisi et al., 2015) which are critical for evaluating reward value and driving appetitive behaviors (Pauli et al., 2016; Voorn et al., 2004).

The early establishment of BNST connectivity with the amygdala, hippocampus, and ventral striatum may provide a foundational basis for later-emerging functions and the early presence of these connections suggests that the BNST may play a role in threat processing and valence surveillance from a very early stage. However, in our 1-month-old sample, we did not observe functional connectivity between the BNST and cortical regions, such as the medial prefrontal cortex (mPFC), which have been consistently reported in resting state functional connectivity studies in youth (Feola et al., 2021) and adults (Avery et al., 2014; Gorka et al., 2018; Motzkin et al., 2015; Tillman et al., 2018; Torrisi et al., 2015; Weis et al., 2019) and structural connectivity studies (Avery et al., 2014; Krüger et al., 2015). BNST–prefrontal connections may support the its interface between higher cognitive functions (Avery et al., 2014; Glover et al., 2020), and their absence in the current study may indicate that long-range BNST connections involving higher-order cortical areas may develop later in development, reflecting the prolonged maturation of prefrontal and associative networks (Kolk and Rakic, 2022). Note that in the current study, we used a conservative approach with Bonferroni voxel-wise correction for multiple comparisons. For visualization purposes, functional connectivity patterns are displayed following a slightly more liberal FDR correction (see Fig. 2), in which we observed a cluster in the mPFC. This may suggest that BNST–mPFC connectivity may be present but remains very weak at this stage of development, which should be interpreted with caution, given the lack of statistical robustness under stricter correction methods. Together, the observed functional connectivity in the current study suggest that BNST connectivity is in the early stages of development during infancy and may continue to evolve as neural pathways mature and behavioral functions emerge.

Greater BNST–amygdala connectivity at 1 month of age was significantly associated with fewer anxiety symptoms assessed at 18 months. The BNST and CeA are two highly interconnected structures that form key components of the central extended amygdala (Alheid and Heimer, 1988; de Olmos and Heimer, 1999), playing a critical role in threat-related processing and stress responses (Davis et al., 2010; Fox et al., 2015; Fox and Shackman, 2019). The BNST and CeA work in concert to integrate sensory and contextual information with emotional salience, enabling adaptive responses to uncertain or prolonged threats (Lebow and Chen, 2016). Thus, greater BNST–amygdala connectivity observed in the current study may relate to less anxiety symptoms through a more coordinated system of BNST–amygdala in integrating and evaluation of threat-related signals, likely supporting adaptive responses (Clauss et al., 2019). Conversely, reduced coordinated communication between BNST and amygdala may compromise the regulation of fear responses, thereby increasing susceptibility to anxiety. However, previous studies in older children or adults have reported null (Jin et al., 2023; Weis et al., 2019) or positive associations (Brinkmann et al., 2018; Pedersen et al., 2020) between BNST–amygdala resting state connectivity and anxiety symptoms, which may reflect developmental differences. For instance, these studies examined fully developed circuits in older populations, in which heightened connectivity might indicate hyperactive threat processing in individuals with anxiety. In contrast, our findings at 1 month of age likely capture the early developmental state of these pathways, in which lower connectivity may indicate reduced synchronization and perturbed development. This discrepancy highlights the importance of examining BNST–amygdala connectivity across developmental stages to better understand its role in anxiety risk. More broadly, prior work shows that the BNST and related subcortical networks are experience-sensitive (Banihashemi et al., 2022) and associated with emotion and HPA-axis dysregulation (Awasthi et al., 2020). Our findings extend this literature by suggesting that BNST connectivity shortly after birth may reflect early individual differences within a plastic threat/stress-responsive circuit that could predispose infants to later anxiety or emotion dysregulation—well before behavioral patterns are observable—highlighting its long-term mental-health implications.

It is noteworthy that most infant resting-state fMRI studies linking early connectivity to temperament or later psychopathology have focused on amygdala connectivity (e.g., Graham et al., 2016; Rogers et al., 2017). For example, stronger neonatal amygdala connectivity with the anterior insula and ventral striatum predicted higher fear at 6 months (Graham et al., 2016). Neonatal amygdala–dorsal anterior cingulate connectivity has been associated with generalized anxiety, and amygdala–medial prefrontal connectivity with behavioral inhibition (Rogers et al., 2017). More recent infant work has expanded to large-scale networks (e.g., Banihashemi et al., 2023; Phillips et al., 2021). For instance, at 3 months, greater amygdala–salience network connectivity (and lower connectivity with the executive control network) mediated the association between higher caregiver depression/trait anxiety and reduced infant positive emotionality (Phillips et al., 2021). Convergent human and animal work indicates that the amygdala supports implicit emotional learning (e.g., fear conditioning) and contributes to emotional modulation of memory, attention and perception, social–emotional behavior, and inhibition/regulation (Phelps and LeDoux, 2005). Our findings extend this literature by showing that circuitry within the extended amygdala—particularly BNST–amygdala connectivity—is prospectively associated with anxiety symptoms in toddlerhood. The BNST–amygdala circuit does not operate in isolation but is embedded within broader salience and regulatory networks (Lebow and Chen, 2016), and healthy emotional development likely reflects maturation of this system. Future work that extends to the broader circuitry can clarify how its components jointly confer risk or resilience.

The absence of a significant association between BNST functional connectivity at 1 month and anxiety risk at 6 months, contrasted with its observed link to anxiety symptoms at 18 months, may reflect differences in developmental timing and the nature of the measures used. At 6 months, emotional regulation and anxiety-related neural processes are still in the early stages of maturation, and the BNST's involvement in sustained threat processing and emotional regulation may not yet be fully operational in the processes underlying the fear temperament assessed by the IBQ. However, by 18 months, emotional and regulatory systems are likely to have undergone further maturation (Casey et al., 2005), enabling a more observable link between early BNST connectivity and anxiety symptoms measured by the ECSA. Another possible explanation for this discrepancy is the developmental and conceptual differences between the measures used at two time points. The IBQ fear subscale at 6 months primarily captures broad temperamental traits such as reactivity to novel or sudden stimuli and distress in unfamiliar social settings (Putnam et al., 2014). In contrast, the ECSA items used at 18 months assess more specific and developmentally later-emerging anxiety-related behaviors, such as situational avoidance, generalized worry, and attachment-related anxiety, which may be more closely linked to the BNST's role in threat processing and sustained fear responses.

This study provides novel evidence of intrinsic BNST functional connectivity as early as 1 month of age and its association with emerging anxiety symptoms in infancy—representing, to our knowledge, the first neuroimaging investigation of BNST connectivity in human infants. Despite the strengths, several limitations merit consideration. First, the sample size limits our ability to detect small clusters or clusters with relatively weaker coupling with the BNST, as well as their associations with later anxiety risk. Additionally, the limited sample size constrains our capacity to explore moderating factors such as sex differences in BNST intrinsic functional connectivity patterns. This is particularly relevant since the BNST is anatomically sexually dimorphic, with such structural differences emerging relatively late in development (Allen and Gorski, 1990; Chung et al., 2002). Nonetheless, functional sex differences may precede detectable structural dimorphism and may relate to gender disparity in the prevalence of anxiety and stress-related disorders (Sloan and Kornstein, 2003; Steiner et al., 2005). Second, this study included measures of BNST intrinsic connectivity only at 1 month of age. Longitudinal studies incorporating repeated assessments of BNST connectivity could provide a better understanding of how BNST connectivity develops over time. Third, while the study employed rigorous statistical methods, including Bonferroni correction for multiple comparisons to control false positives, this conservative approach may have reduced sensitivity, potentially limiting the detection of weaker or emerging connectivity patterns. Fourth, the small size of the BNST presents a challenge for accurately capturing its connectivity with the current low-resolution fMRI. Advanced imaging techniques, such as ultra-high-field fMRI, could enhance spatial resolution and enable more precise localization of BNST.

In conclusion, current study provides novel insights into the intrinsic functional connectivity of the BNST in early infancy and its potential role in shaping later anxiety risk. The BNST exhibits functional connectivity with key subcortical regions, including the amygdala, hippocampus, and ventral striatum, as early as 1 month of age, highlighting that these BNST connections are established remarkably early in development and may provide a foundational basis for later-emerging functions. However, BNST connectivity does not yet exhibit adult-like patterns, suggesting ongoing maturation and an early stage in its development. Importantly, BNST–amygdala connectivity at 1 month was associated with anxiety symptoms at 18 months, highlighting its potential as an early index of individual differences in threat processing and stress responsivity that can confer later anxiety risk. Future longitudinal studies with larger samples are needed to validate and extend these findings, exploring how BNST functional connectivity evolves over time and interacts with environmental and genetic factors to influence later anxiety risk.

CRediT authorship contribution statement

Yanbin Niu: Writing – original draft, Visualization, Methodology, Investigation, Formal analysis. **M. Catalina Camacho:** Writing – review & editing, Supervision, Methodology. **Sanjana Ravi:** Project administration, Methodology, Data curation. **Brandon Wallroff:** Methodology. **Joshua Hageman:** Data curation. **Jennifer Urbano Blackford:** Writing – review & editing, Supervision, Methodology, Formal analysis, Conceptualization. **Kathryn L. Humphreys:** Writing – review & editing, Supervision, Funding acquisition, Conceptualization.

Funding

This work was supported by the Jacobs Foundation Early Career Research Fellowship (2017–1261–05); National Science Foundation CAREER Award (2042285); National Institutes of Health (F32 MH132185); John and Polly Sparks Foundation Investigator Award from the Brain and Behavior Research Foundation (29593); Vanderbilt Institute for Clinical and Translational Research Grant (VR53419); Vanderbilt Strong Grant; Vanderbilt Kennedy Center Grant.

Declaration of Competing Interest

The authors declare that they have no known competing financial interests or personal relationships that could have appeared to influence the work reported in this paper.

Appendix A. Supporting information

Supplementary data associated with this article can be found in the online version at doi:10.1016/j.dcn.2025.101638.

Data availability

Data will be made available on request.

References

Aderka, I.M., Hofmann, S.G., Nickerson, A., Hermesh, H., Gilboa-Schechtman, E., Marom, S., 2012. Functional impairment in social anxiety disorder. J. Anxiety Disord. 26, 393–400. https://doi.org/10.1016/j.janxdis.2012.01.003.

Alheid, G., Heimer, L., 1988. New perspectives in basal forebrain organization of special relevance for neuropsychiatric disorders: the striatopallidal, amygdaloid, and corticopetal components of substantia innominata. Neuroscience 27, 1–39. https://doi.org/10.1016/0306-4522(88)90217-5.

Allen, L.S., Gorski, R.A., 1990. Sex difference in the bed nucleus of the stria terminalis of the human brain. J. Comp. Neurol. 302, 697–706. https://doi.org/10.1002/cne.903020402.

Alvarez, R.P., Chen, G., Bodurka, J., Kaplan, R., Grillon, C., 2011. Phasic and sustained fear in humans elicits distinct patterns of brain activity. NeuroImage 55, 389–400. https://doi.org/10.1016/j.neuroimage.2010.11.057.

Andersson, J.L.R., Skare, S., Ashburner, J., 2003. How to correct susceptibility distortions in spin-echo echo-planar images: application to diffusion tensor imaging. NeuroImage 20, 870–888. https://doi.org/10.1016/S1053-8119(03)00336-7.

Arbuckle, J.L., 2013. Full information estimation in the presence of incomplete data. in: Advanced Structural Equation Modeling. Psychology Press, pp. 243–277.

Avants, B.B., Epstein, C.L., Grossman, M., Gee, J.C., 2008. Symmetric diffeomorphic image registration with cross-correlation: Evaluating automated labeling of elderly and neurodegenerative brain. Med. Image Anal. Spec. Issue Third Int. Workshop Biomed. Image Regist. WBIR 2006 (12), 26–41. https://doi.org/10.1016/j.media.2007.06.004.

Avery, S.N., Clauss, J.A., Blackford, J.U., 2016. The human BNST: Functional role in anxiety and addiction. Neuropsychopharmacol 41, 126–141. https://doi.org/10.1038/npp.2015.185.

Avery, S.N., Clauss, J.A., Winder, D.G., Woodward, N., Heckers, S., Blackford, J.U., 2014. BNST neurocircuitry in humans. NeuroImage 91, 311–323. https://doi.org/10.1016/j.neuroimage.2014.01.017.

Awasthi, S., Pan, H., LeDoux, J.E., Cloitre, M., Altemus, M., McEwen, B., Silbersweig, D., Stern, E., 2020. The bed nucleus of the stria terminalis and functionally linked neurocircuitry modulate emotion processing and HPA axis dysfunction in posttraumatic stress disorder. NeuroImage Clin. 28, 102442. https://doi.org/10.1016/j.nicl.2020.102442.

Banihashemi, L., Peng, C.W., Rangarajan, A., Karim, H.T., Wallace, M.L., Sibbach, B.M., Singh, J., Stinley, M.M., Germain, A., Aizenstein, H.J., 2022. Childhood threat is associated with lower resting-state connectivity within a central visceral network. Front. Psychol. 13, 805049. https://doi.org/10.3389/fpsyg.2022.805049.

Banihashemi, L., Schmithorst, V.J., Bertocci, M.A., Samolyk, A., Zhang, Y., Santos, J.P.L., Versace, A., Taylor, M., English, G., Northrup, J.B., others, 2023. Neural network functional interactions mediate or suppress white matter–emotional behavior relationships in infants. Biol. Psychiatry 94, 57–67. https://doi.org/10.1016/j.biopsych.2023.03.004.

Baughman, N., Prescott, S.L., Rooney, R., 2020. The prevention of anxiety and depression in early childhood. Front. Psychol. 11, 517896. https://doi.org/10.3389/fpsyg.2020.517896.

Bayer, S.A., 1987. Neurogenetic and morphogenetic heterogeneity in the bed nucleus of the stria terminalis. J. Comp. Neurol. 265, 47–64. https://doi.org/10.1002/cne.902650105.

Berry, S.C., Lawrence, A.D., Lancaster, T.M., Casella, C., Aggleton, J.P., Postans, M., 2022. Subiculum–BNST structural connectivity in humans and macaques. NeuroImage 253, 119096. https://doi.org/10.1016/j.neuroimage.2022.119096.

Bienkowski, M.S., Bowman, I., Song, M.Y., Gou, L., Ard, T., Cotter, K., Zhu, M., Benavidez, N.L., Yamashita, S., Abu-Jaber, J., others, 2018. Integration of gene expression and brain-wide connectivity reveals the multiscale organization of mouse hippocampal networks. Nat. Neurosci. 21, 1628–1643. https://doi.org/10.1038/s41593-018-0241-y.

Birn, R.M., Shackman, A.J., Oler, J.A., Williams, L.E., McFarlin, D.R., Rogers, G.M., Shelton, S.E., Alexander, A.L., Pine, D.S., Slattery, M.J., others, 2014. Evolutionarily conserved prefrontal-amygdalar dysfunction in early-life anxiety. Mol. Psychiatry 19, 915–922. https://doi.org/10.1038/mp.2014.46.

Brinkmann, L., Buff, C., Feldker, K., Neumeister, P., Heitmann, C.Y., Hofmann, D., Bruchmann, M., Herrmann, M.J., Straube, T., 2018. Inter-individual differences in trait anxiety shape the functional connectivity between the bed nucleus of the stria terminalis and the amygdala during brief threat processing. Neuroimage 166, 110–116. https://doi.org/10.1016/j.neuroimage.2017.10.054.

Brinkmann, L., Buff, C., Feldker, K., Tupak, S., Becker, M., Herrmann, M., Straube, T., 2017. Distinct phasic and sustained brain responses and connectivity of amygdala and bed nucleus of the stria terminalis during threat anticipation in panic disorder. Psychol. Med. 47, 2675–2688. https://doi.org/10.1017/S0033291717001192.

Buss, K.A., 2011. Which fearful toddlers should we worry about? Context, fear regulation, and anxiety risk. Dev. Psychol. 47, 804. https://doi.org/10.1037/a0023227.

Camacho, M.C., Quiñones-Camacho, L.E., Perlman, S.B., 2020. Does the child brain rest?: An examination and interpretation of resting cognition in developmental cognitive neuroscience. NeuroImage 212, 116688. https://doi.org/10.1016/j.neuroimage.2020.116688.

Casey, B.J., Tottenham, N., Liston, C., Durston, S., 2005. Imaging the developing brain: what have we learned about cognitive development? Trends Cogn. Sci. 9, 104–110. https://doi.org/10.1016/j.tics.2005.01.011.

Chavanne, A.V., Robinson, O.J., 2021. The overlapping neurobiology of induced and pathological anxiety: A meta-analysis of functional neural activation. AJP 178, 156–164. https://doi.org/10.1176/appi.ajp.2020.19111153.

Chung, W.C., De Vries, G.J., Swaab, D.F., 2002. Sexual differentiation of the bed nucleus of the stria terminalis in humans may extend into adulthood. J. Neurosci. 22, 1027–1033. https://doi.org/10.1523/JNEUROSCI.22-03-01027.2002.

Ciric, R., Rosen, A.F.G., Erus, G., Cieslak, M., Adebimpe, A., Cook, P.A., Bassett, D.S., Davatzikos, C., Wolf, D.H., Satterthwaite, T.D., 2018. Mitigating head motion artifact in functional connectivity MRI. Nat. Protoc. 13, 2801–2826. https://doi.org/10.1038/s41596-018-0065-y.

Clancy, B., Darlington, R.B., Finlay, B.L., 2001. Translating developmental time across mammalian species. Neuroscience 105, 7–17. https://doi.org/10.1016/S0306-4522(01)00171-3.

Clauss, J.A., Avery, S.N., Benningfield, M.M., Blackford, J.U., 2019. Social anxiety is associated with BNST response to unpredictability. Depress Anxiety 36, 666–675. https://doi.org/10.1002/da.22891.

Clauss, J.A., Blackford, J.U., 2012. Behavioral inhibition and risk for developing social anxiety disorder: A meta-analytic study. J. Am. Acad. Child Adolesc. Psychiatry 51, 1066–1075.e1. https://doi.org/10.1016/j.jaac.2012.08.002.

Cooke, B.M., Simerly, R.B., 2005. Ontogeny of bidirectional connections between the medial nucleus of the amygdala and the principal bed nucleus of the stria terminalis in the rat. J. Comp. Neurol. 489, 42–58. https://doi.org/10.1002/cne.20612.

Cox, R.W., Chen, G., Glen, D.R., Reynolds, R.C., Taylor, P.A., 2017a. fMRI clustering and false-positive rates. Proc. Natl. Acad. Sci. USA 114, E3370–E3371. https://doi.org/10.1073/pnas.1614961114.

Cox, R.W., Chen, G., Glen, D.R., Reynolds, R.C., Taylor, P.A., 2017b. FMRI clustering in AFNI: False-positive rates redux. Brain Connect 7, 152–171. https://doi.org/10.1089/brain.2016.0475.

Cox, R.W., Hyde, J.S., 1997. Software tools for analysis and visualization of fMRI data. NMR Biomed. 10, 171–178. https://doi.org/10.1002/(SICI)1099-1492(199706/08)10:4/5<171::AID-NBM453>3.0.CO;2-L.

Damoiseaux, J.S., Rombouts, S.A., Barkhof, F., Scheltens, P., Stam, C.J., Smith, S.M., Beckmann, C.F., 2006. Consistent resting-state networks across healthy subjects. Proc. Natl. Acad. Sci. 103, 13848–13853. https://doi.org/10.1073/pnas.0601417103.

Davis, M., Walker, D.L., Miles, L., Grillon, C., 2010. Phasic vs sustained fear in rats and humans: Role of the extended amygdala in fear vs anxiety. Neuropsychopharmacol 35, 105–135. https://doi.org/10.1038/npp.2009.109.

Dong, H.-W., Petrovich, G.D., Swanson, L.W., 2001a. Topography of projections from amygdala to bed nuclei of the stria terminalis. Brain Res. Rev. 38, 192–246. https://doi.org/10.1016/S0165-0173(01)00079-0.

Dong, H.-W., Petrovich, G.D., Watts, A.G., Swanson, L.W., 2001b. Basic organization of projections from the oval and fusiform nuclei of the bed nuclei of the stria terminalis in adult rat brain. J. Comp. Neurol. 436, 430–455. https://doi.org/10.1002/cne.1079.

Dong, H.-W., Swanson, L.W., 2003. Projections from the rhomboid nucleus of the bed nuclei of the stria terminalis: implications for cerebral hemisphere regulation of ingestive behaviors. J. Comp. Neurol. 463, 434–472. https://doi.org/10.1002/cne.10758.

Dong, H.-W., Swanson, L.W., 2004. Organization of axonal projections from the anterolateral area of the bed nuclei of the stria terminalis. J. Comp. Neurol. 468, 277–298. https://doi.org/10.1002/cne.10949.

Dong, H.-W., Swanson, L.W., 2006. Projections from bed nuclei of the stria terminalis, dorsomedial nucleus: implications for cerebral hemisphere integration of neuroendocrine, autonomic, and drinking responses. J. Comp. Neurol. 494, 75–107. https://doi.org/10.1002/cne.20790.

Doria, V., Beckmann, C.F., Arichi, T., Merchant, N., Groppo, M., Turkheimer, F.E., Counsell, S.J., Murgasova, M., Aljabar, P., Nunes, R.G., Larkman, D.J., Rees, G., Edwards, A.D., 2010. Emergence of resting state networks in the preterm human brain. Proc. Natl. Acad. Sci. 107, 20015–20020. https://doi.org/10.1073/pnas.1007921107.

Esteban, O., Markiewicz, C.J., Blair, R.W., Moodie, C.A., Isik, A.I., Erramuzpe, A., Kent, J. D., Goncalves, M., DuPre, E., Snyder, M., Oya, H., Ghosh, S.S., Wright, J., Durnez, J., Poldrack, R.A., Gorgolewski, K.J., 2019. fMRIPrep: a robust preprocessing pipeline for functional MRI. Nat. Methods 16, 111–116. https://doi.org/10.1038/s41592-018-0235-4.

Esteban, O., Markiewicz, C.J., Burns, C., Goncalves, M., Jarecka, D., Ziegler, E., Berleant, S., Ellis, D.G., Pinsard, B., Madison, C., Waskom, M., Notter, M.P., Clark, Daniel, Manhães-Savio, A., Clark, Dav, Jordan, K., Dayan, M., Halchenko, Y. O., Loney, F., Norgaard, M., Salo, T., Dewey, B.E., Johnson, H., Bougacha, S., Keshavan, A., Yvernault, B., Hamalainen, C., Christian, H., Ćirić, R., Dubois, M., Joseph, M., Cipollini, B., Tilley, I.I., S., Visconti di Oleggio Castello, M., De La Vega, A., Wong, J., Kaczmarzyk, J., Huntenburg, J.M., Clark, M.G., Kent, J.D., Benderoff, E., Erickson, D., Dias, M., de, F., Hanke, M., Giavasis, S., Moloney, B., Nichols, B.N., Tungaraza, R., Dell'Orco, A., Frohlich, C., Wassermann, D., de Hollander, G., Koudoro, S., Eshaghi, A., Millman, J., Mancini, M., Close, T., Nielson, D.M., Varoquaux, G., Waller, L., Watanabe, A., Mordom, D., Guillon, J., Robert-Fitzgerald, T., Chetverikov, A., Rokem, A., Acland, B., Forbes, J., Markello, R., Gillman, A., Bernardoni, F., Kong, X.-Z., Geisler, D., Salvatore, J., Gramfort, A., Doll, A., Buchanan, C., DuPre, E., Liu, S., Schaefer, A., Kleesiek, J., Sikka, S., Schwartz, Y., Ghayoor, A., Lee, J.A., Mattfeld, A., Richie-Halford, A., Liem, F., Vaillant, G., Perez-Guevara, M.F., Heinsfeld, A.S., Haselgrove, C., Durnez, J., Lampe, L., Poldrack, R., Glatard, T., Baratz, Z., Tabas, A., Cumba, C., Pérez-García, F., Blair, R., Iqbal, S., Welch, D., Ben-Zvi, G., Contier, O., Triplett, W., Craddock, R.C., Correa, C., Papadopoulos Orfanos, D., Stadler, J., Warner, J., Sisk, L. M., Falkiewicz, M., Sharp, P., Rothmei, S., Kim, S., Weinstein, A., Kahn, A.E., Kastman, E., Bottenhorn, K., Grignard, M., Perkins, L.N., Zhou, D., Bielievtsov, D., Cooper, G., Stojic, H., Hui Qian, T., Linkersdörfer, J., Renfro, M., Hinds, O., Stanley, O., Küttner, R., Pauli, W.M., Xie, X., Glen, D., Kimbler, A., Meyers, B., Tarbert, C., Ginsburg, D., Haehn, D., Margulies, D.S., Condamine, E., Ma, F., Malone, I.B., Snoek, L., Brett, M., Cieslak, M., Hallquist, M., Molina-Romero, M., Bilgel, M., Lee, N., Kuntke, P., Jalan, R., Inati, S., Gerhard, S., Mathotaarachchi, S., Saase, V., Van, A., Steele, C.J., Ort, E., Lerma-Usabiaga, G., Schwabacher, I., Arias, J., Lai, J., Pellman, J., Huguet, J., WEN, J., Leinweber, K., Chawla, K., Weninger, L., Modat, M., Mukhometzianov, R., Harms, R., Andberg, S.K., Matsubara, K., González Orozco, A.A., Routier, A., Marina, A., Davison, A., Floren, A., Park, A., Frederick, B., Cheung, B., McDermottroe, C., McNamee, D., Shachnev, D., Vogel, D., Flandin, G., Jones, H., Gonzalez, I., Varada, J., Schlamp, K., Podranski, K., Huang, L., Noel, M., Pannetier, N., Numssen, O., Khanuja, R., Urchs, S., Shim, S., Nickson, T., Huang, L., Broderick, W., Tambini, A., Mihai, P.G., Gorgolewski, K.J., Ghosh, S., 2022. nipy/nipype: 1.8.3. https://doi.org/10.5281/zenodo.6834519.

Fallucco, E.M., Wysocki, T., James, L., Kozikowski, C., Williams, A., Gleason, M.M., 2017. The brief early childhood screening assessment: Preliminary validity in pediatric primary care. J. Dev. Behav. Pediatr. 38, 89–98. https://doi.org/10.1097/DBP.0000000000000384.

Feola, B., Melancon, S.N.T., Clauss, J.A., Noall, M.P., Mgboh, A., Flook, E.A., Benningfield, M.M., Blackford, J.U., 2021. Bed nucleus of the stria terminalis and amygdala responses to unpredictable threat in children. Dev. Psychobiol. 63, e22206. https://doi.org/10.1002/dev.22206.

Figel, B., Brinkmann, L., Buff, C., Heitmann, C.Y., Hofmann, D., Bruchmann, M., Becker, M.P., Herrmann, M.J., Straube, T., 2019. Phasic amygdala and BNST activation during the anticipation of temporally unpredictable social observation in social anxiety disorder patients. NeuroImage Clin. 22, 101735. https://doi.org/10.1016/j.nicl.2019.101735.

Filippi, C.A., Ravi, S., Bracy, M., Winkler, A., Sylvester, C.M., Pine, D.S., Fox, N.A., 2021. Amygdala functional connectivity and negative reactive temperament at age 4 months. J. Am. Acad. Child Adolesc. Psychiatry 60, 1137–1146. https://doi.org/10.1016/j.jaac.2020.11.021.

Fonov, V., Evans, A., McKinstry, R., Almli, C., Collins, D., 2009. Unbiased nonlinear average age-appropriate brain templates from birth to adulthood. NeuroImage Organ. Hum. Brain Mapp. 2009 Annu. Meet. 47, S102. https://doi.org/10.1016/S1053-8119(09)70884-5.

Fox, A.S., Oler, J.A., Birn, R.M., Shackman, A.J., Alexander, A.L., Kalin, N.H., 2018. Functional connectivity within the primate extended amygdala is heritable and associated with early-life anxious temperament. J. Neurosci. 38, 7611–7621. https://doi.org/10.1523/JNEUROSCI.0102-18.2018.

Fox, A.S., Oler, J.A., Tromp, D.P., Fudge, J.L., Kalin, N.H., 2015. Extending the amygdala in theories of threat processing. Trends Neurosci. 38, 319–329. https://doi.org/10.1016/j.tins.2015.03.002.

Fox, N.A., Pine, D.S., 2012. Temperament and the emergence of anxiety disorders. J. Am. Acad. Child Adolesc. Psychiatry 51, 125–128. https://doi.org/10.1016/j.jaac.2011.10.006.

Fox, A.S., Shackman, A.J., 2019. The central extended amygdala in fear and anxiety: Closing the gap between mechanistic and neuroimaging research. Neurosci. Lett. Funct. Neuroimaging Emot. Brain 693, 58–67. https://doi.org/10.1016/j.neulet.2017.11.056.

Fransson, P., Skiöld, B., Horsch, S., Nordell, A., Blennow, M., Lagercrantz, H., Åden, U., 2007. Resting-state networks in the infant brain. Proc. Natl. Acad. Sci. 104, 15531–15536. https://doi.org/10.1073/pnas.0704380104.

Gelman, A., 2008. Scaling regression inputs by dividing by two standard deviations. Stat. Med. 27, 2865–2873. https://doi.org/10.1002/sim.3107.

Glover, L.R., McFadden, K.M., Bjorni, M., Smith, S.R., Rovero, N.G., Oreizi-Esfahani, S., Yoshida, T., Postle, A.F., Nonaka, M., Halladay, L.R., others, 2020. A prefrontal-bed nucleus of the stria terminalis circuit limits fear to uncertain threat. Elife 9, e60812. https://doi.org/10.7554/eLife.60812.

Gorgolewski, K., Burns, C., Madison, C., Clark, D., Halchenko, Y., Waskom, M., Ghosh, S., 2011. Nipype: a flexible, lightweight and extensible neuroimaging data processing framework in python. Front. Neuroinformatics 5. https://doi.org/10.3389/fninf.2011.00013.

Gorka, A.X., Torrisi, S., Shackman, A.J., Grillon, C., Ernst, M., 2018. Intrinsic functional connectivity of the central nucleus of the amygdala and bed nucleus of the stria terminalis. Neuroimage 168, 392–402. https://doi.org/10.1016/j.neuroimage.2017.03.007.

Graham, A.M., Buss, C., Rasmussen, J.M., Rudolph, M.D., Demeter, D.V., Gilmore, J.H., Styner, M., Entringer, S., Wadhwa, P.D., Fair, D.A., 2016. Implications of newborn amygdala connectivity for fear and cognitive development at 6-months-of-age. Dev. Cogn. Neurosci. Flux Congr. 2014 18, 12–25. https://doi.org/10.1016/j.dcn.2015.09.006.

Greve, D.N., Fischl, B., 2009. Accurate and robust brain image alignment using boundary-based registration. NeuroImage 48, 63–72. https://doi.org/10.1016/j.neuroimage.2009.06.060.

Grogans, S.E., Hur, J., Barstead, M.G., Anderson, A.S., Islam, S., Kim, H.C., Kuhn, M., Tillman, R.M., Fox, A.S., Smith, J.F., DeYoung, K.A., Shackman, A.J., 2024. Neuroticism/negative emotionality is associated with increased reactivity to uncertain threat in the bed nucleus of the stria terminalis, not the amygdala. J. Neurosci. 44. https://doi.org/10.1523/JNEUROSCI.1868-23.2024.

Halladay, L.R., Herron, S.M., 2023. Lasting impact of postnatal maternal separation on the developing BNST: Lifelong socioemotional consequences. Neuropharmacology 225, 109404. https://doi.org/10.1016/j.neuropharm.2022.109404.

Harris, P.A., Taylor, R., Minor, B.L., Elliott, V., Fernandez, M., O'Neal, L., McLeod, L., Delacqua, G., Delacqua, F., Kirby, J., Duda, S.N., 2019. The REDCap consortium: building an international community of software platform partners. J. Biomed. Inform. 95, 103208. https://doi.org/10.1016/j.jbi.2019.103208.

Harris, P.A., Taylor, R., Thielke, R., Payne, J., Gonzalez, N., Conde, J.G., 2009. Research electronic data capture (REDCap)—a metadata-driven methodology and workflow process for providing translational research informatics support. J. Biomed. Inform. 42, 377–381. https://doi.org/10.1016/j.jbi.2008.08.010.

Hofmann, D., Straube, T., 2021. Effective connectivity between bed nucleus of the stria terminalis and amygdala: Reproducibility and relation to anxiety. Hum. Brain Mapp. 42, 824–836. https://doi.org/10.1002/hbm.25265.

Huber, P.J., 1967. The behavior of maximum likelihood estimates under nonstandard conditions. Proceedings of the Fifth Berkeley Symposium on Mathematical Statistics and Probability. University of California Press, Berkeley, CA, pp. 221–233. https://doi.org/10.1515/9783112557563-035.

Jenkinson, M., Bannister, P., Brady, M., Smith, S., 2002. Improved optimization for the robust and accurate linear registration and motion correction of brain images. NeuroImage 17, 825–841. https://doi.org/10.1006/nimg.2002.1132.

Jenkinson, M., Beckmann, C.F., Behrens, T.E., Woolrich, M.W., Smith, S.M., 2012. Fsl. Neuroimage 62, 782–790. https://doi.org/10.1016/j.neuroimage.2011.09.015.

Jenks, S.K., Zhang, S., Chiang-shan, R.L., Hu, S., 2020. Threat bias and resting state functional connectivity of the amygdala and bed nucleus stria terminalis. J. Psychiatr. Res. 122, 54–63. https://doi.org/10.1016/j.jpsychires.2019.12.017.

Jin, S., Liu, W., Hu, Y., Liu, Z., Xia, Y., Zhang, X., Ding, Y., Zhang, L., Xie, S., Ma, C., others, 2023. Aberrant functional connectivity of the bed nucleus of the stria terminalis and its age dependence in children and adolescents with social anxiety disorder. Asian J. Psychiatry 82, 103498. https://doi.org/10.1016/j.ajp.2023.103498.

Kessler, R.C., Berglund, P., Demler, O., Jin, R., Merikangas, K.R., Walters, E.E., 2005. Lifetime prevalence and age-of-onset distributions of DSM-IV disorders in the National Comorbidity Survey Replication. Arch. Gen. Psychiatry 62, 593–602. https://doi.org/10.1001/archpsyc.62.6.593.

Kessler, R.C., Petukhova, M., Sampson, N.A., Zaslavsky, A.M., Wittchen, H.-U., 2012. Twelve-month and lifetime prevalence and lifetime morbid risk of anxiety and mood disorders in the United States. Int. J. Methods Psychiatr. Res. 21, 169–184. https://doi.org/10.1002/mpr.1359.

Klumpers, F., Kroes, M.C., Baas, J.M., Fernández, G., 2017. How human amygdala and bed nucleus of the stria terminalis may drive distinct defensive responses. J. Neurosci. 37, 9645–9656. https://doi.org/10.1523/JNEUROSCI.3830-16.2017.

Kolk, S.M., Rakic, P., 2022. Development of prefrontal cortex. Neuropsychopharmacology 47, 41–57. https://doi.org/10.1038/s41386-021-01137-9.

Kostović, I., Sedmak, G., Judaš, M., 2019. Neural histology and neurogenesis of the human fetal and infant brain. NeuroImage 188, 743–773. https://doi.org/10.1016/j.neuroimage.2018.12.043.
Krüger, O., Shiozawa, T., Kreifelts, B., Scheffler, K., Ethofer, T., 2015. Three distinct fiber pathways of the bed nucleus of the stria terminalis to the amygdala and prefrontal cortex. Cortex 66, 60–68. https://doi.org/10.1016/j.cortex.2015.02.007.
Lanczos, C., 1964. Evaluation of noisy data. J. Soc. Ind. Appl. Math. Ser. B Numer. Anal. 1, 76–85. https://doi.org/10.1137/0701007.
Lanzillo, M., Gervais, M., Croizier, S., 2021. Ontogeny of the projections from the dorsomedial division of the anterior bed nucleus of the stria terminalis to hypothalamic nuclei. Front. Neurosci. 15, 748186. https://doi.org/10.3389/fnins.2021.748186.
Lebow, M.A., Chen, A., 2016. Overshadowed by the amygdala: the bed nucleus of the stria terminalis emerges as key to psychiatric disorders. Mol. Psychiatry 21, 450–463. https://doi.org/10.1038/mp.2016.1.
McKnight, P.E., Monfort, S.S., Kashdan, T.B., Blalock, D.V., Calton, J.M., 2016. Anxiety symptoms and functional impairment: A systematic review of the correlation between the two measures. Clin. Psychol. Rev. 45, 115–130. https://doi.org/10.1016/j.cpr.2015.10.005.
Mendlowicz, M.V., Stein, M.B., 2000. Quality of life in individuals with anxiety disorders. Am. J. Psychiatry 157, 669–682. https://doi.org/10.1176/appi.ajp.157.5.669.
Meyer, C., Padmala, S., Pessoa, L., 2019. Dynamic threat processing. J. Cogn. Neurosci. 31, 522–542. https://doi.org/10.1162/jocn_a_01363.
Mori, S., Aggarwal, M., 2014. In vivo magnetic resonance imaging of the human limbic white matter. Front. Aging Neurosci. 6, 321. https://doi.org/10.3389/fnagi.2014.00321.
Motzkin, J.C., Philippi, C.L., Oler, J.A., Kalin, N.H., Baskaya, M.K., Koenigs, M., 2015. Ventromedial prefrontal cortex damage alters resting blood flow to the bed nucleus of stria terminalis. cortex 64, 281–288. https://doi.org/10.1016/j.cortex.2014.11.013.
Murphy, K., Birn, R.M., Handwerker, D.A., Jones, T.B., Bandettini, P.A., 2009. The impact of global signal regression on resting state correlations: Are anti-correlated networks introduced? NeuroImage 44, 893–905. https://doi.org/10.1016/j.neuroimage.2008.09.036.
Murphy, K., Fox, M.D., 2017. Towards a consensus regarding global signal regression for resting state functional connectivity MRI. NeuroImage Clean. fMRI Time Ser. Mitigating noise Adv. Acquis. Correct. Strateg. 154, 169–173. https://doi.org/10.1016/j.neuroimage.2016.11.052.
Myers, B., Mark Dolgas, C., Kasckow, J., Cullinan, W.E., Herman, J.P., 2014. Central stress-integrative circuits: forebrain glutamatergic and GABAergic projections to the dorsomedial hypothalamus, medial preoptic area, and bed nucleus of the stria terminalis. Brain Struct. Funct 219, 1287–1303. https://doi.org/10.1007/s00429-013-0566-y.
Nauta, W.J., Nauta, W., 1993. Fibre degeneration following lesions of the amygdaloid complex in the monkey. Neuroanatomy 202–219. https://doi.org/10.1007/978-1-4684-7920-1_12.
Nielsen, A.N., Kaplan, S., Meyer, D., Alexopoulos, D., Kenley, J.K., Smyser, T.A., Wakschlag, L.S., Norton, E.S., Raghuraman, N., Warner, B.B., Shimony, J.S., Luby, J.L., Neil, J.J., Petersen, S.E., Barch, D.M., Rogers, C.E., Sylvester, C.M., Smyser, C.D., 2023. Maturation of large-scale brain systems over the first month of life. Cereb. Cortex 33, 2788–2803. https://doi.org/10.1093/cercor/bhac242.
Oler, J.A., Birn, R.M., Patriat, R., Fox, A.S., Shelton, S.E., Burghy, C.A., Stodola, D.E., Essex, M.J., Davidson, R.J., Kalin, N.H., 2012. Evidence for coordinated functional activity within the extended amygdala of non-human and human primates. Neuroimage 61, 1059–1066. https://doi.org/10.1016/j.neuroimage.2012.03.045.
Oler, J.A., Tromp, D.P.M., Fox, A.S., Kovner, R., Davidson, R.J., Alexander, A.L., McFarlin, D.R., Birn, R.M., E. Berg, B., deCampo, D.M., Kalin, N.H., Fudge, J.L., 2017. Connectivity between the central nucleus of the amygdala and the bed nucleus of the stria terminalis in the non-human primate: neuronal tract tracing and developmental neuroimaging studies. Brain Struct. Funct. 222, 21–39. https://doi.org/10.1007/s00429-016-1198-9.
de Olmos, J.S., Heimer, L., 1999. The concepts of the ventral striatopallidal system and extended amygdala. Ann. N. Y. Acad. Sci. 877, 1–32. https://doi.org/10.1111/j.1749-6632.1999.tb09258.x.
Pauli, W.M., O'Reilly, R.C., Yarkoni, T., Wager, T.D., 2016. Regional specialization within the human striatum for diverse psychological functions. Proc. Natl. Acad. Sci. 113, 1907–1912. https://doi.org/10.1073/pnas.1507610113.
Pedersen, W.S., Schaefer, S.M., Gresham, L.K., Lee, S.D., Kelly, M.P., Mumford, J.A., Oler, J.A., Davidson, R.J., 2020. Higher resting-state BNST-CeA connectivity is associated with greater corrugator supercilii reactivity to negatively valenced images. NeuroImage 207, 116428. https://doi.org/10.1016/j.neuroimage.2019.116428.
Phelps, E.A., LeDoux, J.E., 2005. Contributions of the amygdala to emotion processing: from animal models to human behavior. Neuron 48, 175–187. https://doi.org/10.1016/j.neuron.2005.09.025.
Phillips, M.L., Schmithorst, V.J., Banihashemi, L., Taylor, M., Samolyk, A., Northrup, J.B., English, G.E., Versace, A., Stiffler, R.S., Aslam, H.A., others, 2021. Patterns of infant amygdala connectivity mediate the impact of high caregiver affect on reducing infant smiling: Discovery and replication. Biol. Psychiatry 90, 342–352. https://doi.org/10.1016/j.biopsych.2021.03.026.
Power, J.D., Mitra, A., Laumann, T.O., Snyder, A.Z., Schlaggar, B.L., Petersen, S.E., 2014. Methods to detect, characterize, and remove motion artifact in resting state fMRI. NeuroImage 84, 320–341. https://doi.org/10.1016/j.neuroimage.2013.08.048.
Putnam, S.P., Helbig, A.L., Gartstein, M.A., Rothbart, M.K., Leerkes, E., 2014. Development and assessment of short and very short forms of the infant behavior questionnaire–revised. J. Personal. Assess. 96, 445–458. https://doi.org/10.1080/00223891.2013.841171.
R Core Team, 2013. R: A language and environment for statistical computing.
Rabellino, D., Densmore, M., Harricharan, S., Jean, T., McKinnon, M.C., Lanius, R.A., 2018. Resting-state functional connectivity of the bed nucleus of the stria terminalis in post-traumatic stress disorder and its dissociative subtype. Hum. Brain Mapp. 39, 1367–1379. https://doi.org/10.1002/hbm.23925.
Ravi, S., Catalina Camacho, M., Fleming, B., Scudder, M.R., Humphreys, K.L., 2023. Concurrent and prospective associations between infant frontoparietal and default mode network connectivity and negative affectivity. Biol. Psychol. 184, 108717. https://doi.org/10.1016/j.biopsycho.2023.108717.
Rinaman, L., Levitt, P., Card, J.P., 2000. Progressive postnatal assembly of limbic–autonomic circuits revealed by central transneuronal transport of pseudorabies virus. J. Neurosci. 20, 2731–2741. https://doi.org/10.1523/JNEUROSCI.20-07-02731.2000.
Rogers, C.E., Sylvester, C.M., Mintz, C., Kenley, J.K., Shimony, J.S., Barch, D.M., Smyser, C.D., 2017. Neonatal amygdala functional connectivity at rest in healthy and preterm infants and early internalizing symptoms. J. Am. Acad. Child Adolesc. Psychiatry 56, 157–166. https://doi.org/10.1016/j.jaac.2016.11.005.
Rosenfeld, A., 1976. Digital picture processing. Academic press.
Salzwedel, A.P., Stephens, R.L., Goldman, B.D., Lin, W., Gilmore, J.H., Gao, W., 2019. Development of amygdala functional connectivity during infancy and its relationship with 4-Year behavioral outcomes. Biological Psychiatry Cognitive Neuroscience Neuroimaging 4, 62–71. https://doi.org/10.1016/j.bpsc.2018.08.010.
Satterthwaite, T.D., Elliott, M.A., Gerraty, R.T., Ruparel, K., Loughead, J., Calkins, M.E., Eickhoff, S.B., Hakonarson, H., Gur, R.C., Gur, R.E., Wolf, D.H., 2013. An improved framework for confound regression and filtering for control of motion artifact in the preprocessing of resting-state functional connectivity data. NeuroImage 64, 240–256. https://doi.org/10.1016/j.neuroimage.2012.08.052.
Shackman, A.J., Fox, A.S., 2016. Contributions of the central extended amygdala to fear and anxiety. J. Neurosci. 36, 8050–8063. https://doi.org/10.1523/JNEUROSCI.0982-16.2016.
Sherbourne, C., Sullivan, G., Craske, M.G., Roy-Byrne, P., Golinelli, D., Rose, R.D., Chavira, D.A., Bystritsky, A., Stein, M.B., 2010. Functioning and disability levels in primary care out-patients with one or more anxiety disorders. Psychol. Med. 40, 2059–2068. https://doi.org/10.1017/S0033291710000176.
Shin, J.-W., Geerling, J.C., Loewy, A.D., 2008. Inputs to the ventrolateral bed nucleus of the stria terminalis. J. Comp. Neurol. 511, 628–657. https://doi.org/10.1002/cne.21870.
Siminski, N., Böhme, S., Zeller, J., Becker, M., Bruchmann, M., Hofmann, D., Breuer, F., Mühlberger, A., Schiele, M., Weber, H., others, 2021. BNST and amygdala activation to threat: Effects of temporal predictability and threat mode. Behav. brain Res. 396, 112883. https://doi.org/10.1016/j.bbr.2020.112883.
Sloan, D.M., Kornstein, S.G., 2003. Gender differences in depression and response to antidepressant treatment. Psychiatr. Clin. 26, 581–594. https://doi.org/10.1016/S0193-953X(03)00044-3.
Somerville, L.H., Whalen, P.J., Kelley, W.M., 2010. Human bed nucleus of the stria terminalis indexes hypervigilant threat monitoring. Biol. Psychiatry Stress Neuroplast. Post. Stress Disord. 68, 416–424. https://doi.org/10.1016/j.biopsych.2010.04.002.
Steiner, M., Allgulander, C., Ravindran, A., Kosar, H., Burt, T., Austin, C., 2005. Gender differences in clinical presentation and response to sertraline treatment of generalized anxiety disorder. Hum. Psychopharmacol. Clin. Exp. 20, 3–13. https://doi.org/10.1002/hup.648.
Strange, B.A., Witter, M.P., Lein, E.S., Moser, E.I., 2014. Functional organization of the hippocampal longitudinal axis. Nat. Rev. Neurosci. 15, 655–669. https://doi.org/10.1038/nrn3785.
Swanson, L., Cowan, W., 1977. An autoradiographic study of the organization of the efferet connections of the hippocampal formation in the rat. J. Comp. Neurol. 172, 49–84. https://doi.org/10.1002/cne.901720104.
Theiss, J.D., Ridgewell, C., McHugo, M., Heckers, S., Blackford, J.U., 2017. Manual segmentation of the human bed nucleus of the stria terminalis using 3T MRI. NeuroImage 146, 288–292. https://doi.org/10.1016/j.neuroimage.2016.11.047.
Thomas, E., Buss, C., Rasmussen, J.M., Entringer, S., Ramirez, J.S., Marr, M., Rudolph, M.D., Gilmore, J.H., Styner, M., Wadhwa, P.D., others, 2019. Newborn amygdala connectivity and early emerging fear. Dev. Cogn. Neurosci. 37, 100604. https://doi.org/10.1016/j.dcn.2018.12.002.
Tillman, R.M., Stockbridge, M.D., Nacewicz, B.M., Torrisi, S., Fox, A.S., Smith, J.F., Shackman, A.J., 2018. Intrinsic functional connectivity of the central extended amygdala. Hum. brain Mapp. 39, 1291–1312. https://doi.org/10.1002/hbm.23917.
Torrisi, S., Alvarez, G.M., Gorka, A.X., Fuchs, B., Geraci, M., Grillon, C., Ernst, M., 2019. Resting-state connectivity of the bed nucleus of the stria terminalis and the central nucleus of the amygdala in clinical anxiety. J. Psychiatry Neurosci. 44, 313–323. https://doi.org/10.1503/jpn.180150.
Torrisi, S., O'Connell, K., Davis, A., Reynolds, R., Balderston, N., Fudge, J.L., Grillon, C., Ernst, M., 2015. Resting state connectivity of the bed nucleus of the stria terminalis at ultra-high field. Hum. Brain Mapp. 36, 4076–4088. https://doi.org/10.1002/hbm.22899.
Tustison, N.J., Avants, B.B., Cook, P.A., Zheng, Y., Egan, A., Yushkevich, P.A., Gee, J.C., 2010. N4ITK: improved N3 bias correction. IEEE Trans. Med. Imaging 29, 1310–1320. https://doi.org/10.1109/TMI.2010.2046908.
Voorn, P., Vanderschuren, L.J., Groenewegen, H.J., Robbins, T.W., Pennartz, C.M., 2004. Putting a spin on the dorsal–ventral divide of the striatum. Trends Neurosci. 27, 468–474. https://doi.org/10.1016/j.tins.2004.06.006.

Walker, D.L., Toufexis, D.J., Davis, M., 2003. Role of the bed nucleus of the stria terminalis versus the amygdala in fear, stress, and anxiety. Eur. J. Pharmacol. 463, 199–216. https://doi.org/10.1016/S0014-2999(03)01282-2.

Weis, C.N., Huggins, A.A., Bennett, K.P., Parisi, E.A., Larson, C.L., 2019. High-resolution resting-state functional connectivity of the extended amygdala. Brain Connect. 9, 627–637. https://doi.org/10.1089/brain.2019.0688.

White, H., 1982. Maximum likelihood estimation of misspecified models. Économ. J. Econom. Soc. 1–25. https://doi.org/10.2307/1912526.

Worsley, K.J., Friston, K.J., 1995. Analysis of fMRI time-series revisited—again. Neuroimage 2, 173–181. https://doi.org/10.1006/nimg.1995.1023.

Worsley, K.J., Marrett, S., Neelin, P., Vandal, A.C., Friston, K.J., Evans, A.C., 1996. A unified statistical approach for determining significant signals in images of cerebral activation. Hum. brain Mapp 4, 58–73. https://doi.org/10.1002/(SICI)1097-0193(1996)4:1%3C58::AID-HBM4%3E3.0.CO;2-O.

Yassa, M.A., Hazlett, R.L., Stark, C.E., Hoehn-Saric, R., 2012. Functional MRI of the amygdala and bed nucleus of the stria terminalis during conditions of uncertainty in generalized anxiety disorder. J. Psychiatr. Res. 46, 1045–1052. https://doi.org/10.1016/j.jpsychires.2012.04.013.

Zeidman, P., Maguire, E.A., 2016. Anterior hippocampus: the anatomy of perception, imagination and episodic memory. Nat. Rev. Neurosci. 17, 173–182. https://doi.org/10.1038/nrn.2015.24.

Zöllei, L., Iglesias, J.E., Ou, Y., Grant, P.E., Fischl, B., 2020. Infant FreeSurfer: An automated segmentation and surface extraction pipeline for T1-weighted neuroimaging data of infants 0–2 years. NeuroImage 218, 116946. https://doi.org/10.1016/j.neuroimage.2020.116946.